Polymer Degradation and Stability 93 (2008) 2025–2031

Contents lists available at ScienceDirect

Polymer Degradation and Stability

journal homepage: www.elsevier.com/locate/polydegstab

Preparation, thermal properties and flame retardancy of phosphorus- and silicon-containing epoxy resins

M. Spontón, L.A. Mercado, J.C. Ronda, M. Galià*, V. Cádiz

Departament de Química Analítica i Química Orgànica, Universitat Rovira i Virgili, Campus Sescelades, Marcel.lí Domingo s/n, 43007 Tarragona, Spain

ARTICLE INFO

Article history:
Received 1 February 2008
Received in revised form 12 February 2008
Accepted 21 February 2008
Available online 23 July 2008

Keywords:
Flame retardance
Epoxy
Phosphorus-containing resins
Silicon-containing resins

ABSTRACT

Phosphorus- and silicon-containing epoxy resins were prepared from (2,5-dihydroxyphenyl)diphenyl phosphine oxide (Gly-HPO), diglycidyloxy methylphenyl silane (DGMPS) and 1,4-bis(glycidyloxydimethyl silyl)-benzene (BGDMSB) as epoxy monomers and diaminodiphenylmethane (DDM), bis(3-aminophenyl)methyl phosphine oxide (BAMPO) and bis(4-aminophenoxy)dimethyl silane (APDS) as curing agents. Epoxy resins with different phosphorus and silicon content were obtained. Their thermal, dynamic mechanical and flame retardant properties were evaluated. The high LOI values confirmed that epoxy resins containing hetero-atoms are effective flame retardants, but a synergistic efficiency of phosphorus and silicon on flame retardation was not observed.

1. Introduction

Epoxy resins are used worldwide on a large scale for adhesive, lamination, coating applications, so forth. They have excellent moisture, solvent and chemical resistances, toughness, low shrinkage on cure, high adhesion to many substrates and superior electrical and mechanical resistance properties [1,2]. To extend the applications of epoxy resins as electronic materials and in the aerospace industry, it is crucial to improve their thermal and flame resistance. Several approaches have been reported in the literature for the improvement of flame resistance. Halogenated compounds have been widely used as flame retardant in the past. The major problem encountered with these systems is the fire hazards resulting from the formation of highly toxic and corrosive products during combustion. With safety and environmental concerns in mind, epoxy resins that are flame resistant and halogen-free have been the focus of attention by researchers in recent years [3,4].

A traditional technique of preparing flame retardant epoxy resins is to blend the flame retardant additive with the polymer. As there is no chemical bonding between the flame retardant additive and the polymer, some shortcomings, such as low efficiency of flame retardance, leaking out during processing and usage, and detrimental effects on polymer's thermal and mechanical properties accompany the introduction of flame retardant into the polymer. Therefore, the present trend is moving towards using reactive type flame retardants, which are permanently bonded to the polymer [5]. Preparing a reactive type flame retardant requires developing novel compounds with specific reactive functional groups, as flame retardant oxirane and diamine compounds for epoxy resins. Among non-halogenated flame retardants, phosphorus-containing compounds are attractive owing to their low generation of smoke and toxic gases and the high flame retardant efficiency [6]. Phosphorus-containing polymers confer fire resistance mainly by modifying the thermal decomposition of the polymers, in favour of reactions yielding carbonaceous char rather than CO and CO_2. They form a surface layer of protective char during fire before the unburned material begins to decompose. The char acts as a barrier to inhibit gaseous products from diffusing to the pyrolysis zone and to shield the polymer surface from heat and air [7]. The efficiency of flame retardation of phosphorus basically depends on the amount of char formation, thus, by improving the thermal stability of phosphorus char at high temperatures the flame retardant efficiency could be improved. Silicon-containing polymers are described that can degrade forming thermally stable silica, which have the tendency to migrate to the char surface serving as a protection layer to prevent further degradation of char at high temperatures [8].

Moreover, enhancement of flame retardancy of epoxy resins has been achieved by incorporation of phosphorus and silicon into epoxy resins with bringing a P–Si synergistic effect of flame retardation [9–13]. While under flame exposure, phosphorus provides a tendency for char formation, silicon provides an enhancement of the thermal stability of the char and introducing both elements may successfully combine these two factors in a strong flame retardation mechanism.

In our search for new flame retardant epoxy monomers and curing agents, we considered phosphine oxides. In a previous work, we

* Corresponding author.
E-mail address: marina.galia@urv.cat (M. Galià).

0141-3910/$ – see front matter © 2008 Elsevier Ltd. All rights reserved.
doi:10.1016/j.polymdegradstab.2008.02.014

synthesized the diglycidyl ether of (2,5-dihydroxyphenyl)diphenyl phosphine oxide (Gly-HPO) and investigated its thermal behaviour and reactivity. Systems containing different amounts of Gly-HPO and DGEBA cured with primary amines were also described and their thermal, mechanical and flame retardant properties were discussed [14]. We also investigated silicon-containing compounds as flame retardants: silicon-containing glycidyl monomers and prepolymers have been cured with primary amines and the thermal stability and flame retardant properties have been reported [15]. We described a new silicon-containing monomer, diglycidyloxy methylphenyl silane (DGMPS) and we examined the incorporation of different amounts of silicon into the epoxy resin by the curing of DGMPS/DGEBA system [16]. In the present work, phosphorus and silicon were introduced into the epoxy resins by curing phosphorus and silicon epoxy monomers with diaminodiphenylmethane (DDM) or a phosphorus- or silicon-containing diamines. In this way, the phosphorus and silicon contents of the resins were altered. The degradation behaviours and flame retardant properties were investigated to examine the possibility of phosphorus–silicon synergistic effect.

2. Experimental

2.1. Materials

Methylphenyl silane (Aldrich), 1,4-bis(hydroxydimethyl silyl) benzene (ABCR), bis(dimethylamino)dimethyl silane (ABCR), 4,4′ diaminodiphenylmethane (DDM) (Aldrich), triphenylphosphine (Aldrich), copper(II) chloride (Probus), sodium sulfite (Baker), potassium *tert*-butoxide (Fluka) and Wilkinson catalyst (Aldrich) were used as received. Glycidol (Aldrich) was vacuum distilled over CaH_2 prior to use. *p*-Aminophenol (Fluka) was recrystallised from ethanol. Copper(I) chloride was prepared by the reduction of copper(II) chloride with sodium sulfite. All solvents were purified by standard procedures.

Diglycidyl ether of (2,5-dihydroxyphenyl)diphenyl phosphine oxide (Gly-HPO) was obtained from (2,5-dihydroxyphenyl)diphenyl phosphine oxide by reaction with epichlorohydrin and BTMA as catalyst as has been previously described [14]. Bis(3-aminophenyl)methyl phosphine oxide (BAMPO) was prepared by nitration of diphenylmethyl phosphine oxide and subsequent reduction with HCl and $SnCl_2$ [17].

2.1.1. Synthesis of $[(Ph_3P)CuH]_6$

Triphenylphosphine (31.0 g, 0.12 mol), copper(I) chloride (4.6 g, 0.045 mol) and toluene (200 ml) were added to a dry, septum-capped 500 ml Schlenk flask and placed under argon. The resultant solution was stirred and potassium *tert*-butoxide (5.1 g, 0.45 mol) was added. The yellow mixture was placed under positive pressure of hydrogen and stirred overnight. During this period the solution turned red, then dark red, and some brown material precipitated. The reaction mixture was transferred under argon pressure to a 500 ml flask and 250 ml of pentane was added. The solution was cooled promoting crystallization of the product, which was filtered and washed several times with pentane and toluene and dried under vacuum to give 10.5 g (75% yield) of dark red crystals.

2.1.2. Synthesis of diglycidyloxy methylphenyl silane (DGMPS)

Into a three-necked round bottom flask equipped with a magnetic stirrer, a dropping funnel and a reflux condenser, 30 ml of anhydrous toluene, 12.0 g (0.162 mol) of freshly distilled glycidol and 6.7×10^{-2} g (7.2×10^{-2} mol, 0.05 mol% per Si–H) of Wilkinson catalyst were placed. The red solution was degassed with argon and heated at 60 °C for 30 min, after which 8.8 g (0.072 mol) of methylphenyl silane was added dropwise over 1 h. Vigorous H_2 evolution was observed immediately and the reaction mixture was kept under positive argon pressure during the entire course of the reaction in order to flush the H_2 gas from the reaction mixture. The solution was stirred at 60 °C for 1 h to ensure complete conversion and was allowed to cool down to ambient temperature overnight. The reaction mixture was washed with water and phosphate buffer and the organic layer was dried over $MgSO_4$, filtered and then the solvent was evaporated at reduced pressure. The product obtained was dissolved in hexane/ethyl acetate (8:2) mixture and filtered through a short column of silica gel to remove traces of catalyst and other polar impurities. The obtained colourless solution was concentrated under vacuum to give a clear oil (74% yield) essentially pure by ^{1}H NMR.

^{1}H NMR ($CDCl_3$/TMS, δ (ppm)): 7.65 (2H, m); 7.42 (3H, m); 4.03 (2H, dd, 12.0, 3.2 Hz); 3.75 (2H, dd, 12.0, 5.2 Hz); 3.15 (2H, m); 2.78 (2H, dd, 4.4, 2.8 Hz); 2.65 (2H, dd, 4.4, 2.8 Hz); 0.42 (3H, s).

^{13}C NMR ($CDCl_3$/TMS, δ (ppm)): 134.0 (d); 132.2 (s); 130.4 (d); 127.9 (d); 63.6 (t); 52.0 (d); 44.5 (t); −4.4 (q).

2.1.3. Synthesis of 1,4-bis(glycidyloxydimethyl silyl)-benzene (BGDMSB)

20 ml (22.4 g, 0.3 mol) of glycidol dissolved in 40 ml of anhydrous toluene and 0.3 g (0.5 mol% per Si–H) of copper hydride hexamer catalyst were introduced into a 250 ml Schlenk flask containing a magnetic stirrer and sealed with a rubber septum. The mixture was degassed and infused with argon. 19.5 g (22.4 ml, 0.1 mol) of 1,4-bis(dimethylsilyl benzene) was introduced dropwise into the reaction flask via dropping funnel for 10 min. At this time the reaction solution became red in colour and gas evolution was observed. The reaction mixture was kept at room temperature and after 5 h the reaction was complete. After washing with 5% of NH_3 and water three times and drying with $MgSO_4$, the resulting clear oil was dissolved in hexane/ethyl acetate (9:1) mixture and filtered through a short column of silica gel to remove polar impurities. By concentration under vacuum a colourless oil (78% yield), pure by ^{1}H NMR, was obtained.

^{1}H NMR ($CDCl_3$/TMS, δ (ppm)): 7.58 (4H, s); 3.82 (2H, dd, 12.0, 3.3 Hz); 3.60 (2H, dd, 12.0, 5.4 Hz); 3.09 (2H, m); 2.76 (2H, dd, 5.2, 4.1 Hz); 2.59 (2H, dd, 5.2, 2.9 Hz); 0.42 (12H, s).

^{13}C NMR ($CDCl_3$/TMS, δ (ppm)): 139.7 (s); 132.8 (d); 63.8 (t); 52.1 (d); 44.6 (t); −1.9 (q).

2.1.4. Synthesis of bis(4-aminophenoxy)dimethyl silane (APDS)

Into a three-necked round bottom flask equipped with a magnetic stirrer, a dropping funnel and a reflux condenser, 37.3 g (0.34 mol) of *p*-aminophenol and 100 ml of anhydrous toluene were placed. The mixture reaction was vigorously stirred under argon and heated to 110 °C. Bis(dimethylamino)dimethyl silane (25 g, 0.17 mol) was added dropwise for 60 min. The reaction was kept at this temperature for 36 h until no dimethylamine evolution was observed. The dark yellow suspension was filtered to obtain a yellow solution that was concentrated under vacuum to obtain 40 g of a yellow oil that solidifies on standing overnight. The product was purified by recrystallisation from hexane/ethyl acetate (9:1), and obtained as a yellow solid with a 62% yield.

^{1}H NMR ($CDCl_3$/TMS, δ (ppm)): 6.75 (4H, d); 6.55 (4H, d); 3.43 (4H, s); 0.30 (6H, s).

^{13}C NMR ($CDCl_3$/TMS, δ (ppm)): 146.7 (s); 140.0 (s); 120.3 (d); 116.2 (d); −2.5 (q).

2.2. Curing reactions

The curing conditions were established by Differential Scanning Calorimetry. Samples (Table 1) were prepared by the dissolution of epoxy monomers and curing agent in CH_3OH or CH_2Cl_2. Then this solution was evaporated at room temperature in vacuum. About 5 mg of a known weight of the mixture was put into the aluminium

Table 1
Compositions, phosphorus and silicon content and curing data of the epoxy resins

Sample	Epoxy monomer[a]	Curing agent[b]	P (%)	Si (%)	T_{onset}[c] (°C)	T_{max}[d] (°C)	ΔH_0[e] (Kj/ee)
1	Gly-HPO	DDM	5.9	–	120	150	82
2	Gly-HPO	BAMPO	8.5	–	137	168	95
3	Gly-HPO	APDS	5.5	2.5	112	143	82
4	DGMPS	DDM	–	7.7	120	157	83
5	DGMPS	BAMPO	4.0	7.2	132	172	–
6	DGMPS	APDS	–	10.4	117	145	84
7	BGDMSB	DDM	–	12.8	111	168	83
8	BGDMSB	BAMPO	3.4	12.2	148	196	–
9	BGDMSB	APDS	–	14.7	129	162	83
10	Gly-HPO/DGMPS	DDM	3.5	3.2	119	159	88
11	Gly-HPO/DGMPS	BAMPO	6.6	3.0	136	170	–
12	Gly-HPO/DGMPS	APDS	3.2	5.8	111	142	82
13	Gly-HPO/BGDMSB	DDM	3.2	5.8	117	163	91
14	Gly-HPO/BGDMSB	BAMPO	6.2	5.5	123	170	97
15	Gly-HPO/BGDMSB	APDS	3.0	8.1	114	156	81

[a] For the mixtures of epoxy monomers, a 1:1 mol ratio was used.
[b] Stoichiometric amounts were used in all cases.
[c] Initial temperature of the crosslinking exotherm (10 °C/min).
[d] Temperature of the maximum heat release rate (10 °C/min).
[e] Reaction enthalpy values per epoxy equivalent.

pan, and the polymerization was monitored in a dynamic DSC experiment using a heating rate of 10 °C/min. The curing conditions are shown in Table 2. Moulded epoxy resins for DMTA and LOI measurements were obtained by moulding about 1.5 g of a known weight of the mixture obtained as described above.

2.3. Instrumentation

^1H (300 MHz) and ^{13}C (75.4 MHz) NMR spectra were obtained with a Varian Gemini 300 spectrometer with Fourier Transform, with $CDCl_3$ as a solvent, and with TMS as an internal standard. The IR spectra were obtained with a ATR-FTIR JASCO 680.

Calorimetric studies were carried out on a Mettler DSC821e thermal analyser using N_2 as a purge gas (20 ml/min). Thermal stability studies were carried out on a Mettler TGA/SDTA851e/LF/1100 with N_2 and air as a purge gas at scan rates of 10 °C/min.

Table 2
Curing and post-curing conditions and T_g data of the epoxy resins

Sample	Epoxy monomer[a]	Curing agent[b]	Curing	Post-curing	T_g (°C)		
					½ ΔC_p[c]	E''_{max}[d]	tan δ_{max}[e]
1	Gly-HPO	DDM	120 °C, 2 h	200 °C, 3 h	193	181	193
2	Gly-HPO	BAMPO	140 °C, 2 h	200 °C, 2 h	198	154	194
3	Gly-HPO	APDS	120 °C, 2 h	180 °C, 2 h	167	158	167
4	DGMPS	DDM	105 °C, 2 h	165 °C, 2 h	77	72	87
5	DGMPS	BAMPO	150 °C, 2 h	180 °C, 1 h	75	76	84
6	DGMPS	APDS	120 °C, 3 h	160 °C, 3 h	70	63	70
7	BGDMSB	DDM	120 °C, 2 h	180 °C, 2 h	60	62	64
8	BGDMSB	BAMPO	145 °C, 2 h	195 °C, 2 h	80	90	105
9	BGDMSB	APDS	120 °C, 3 h	180 °C, 2 h	59	53	68
10	Gly-HPO/DGMPS	DDM	120 °C, 2 h	180 °C, 2 h	125	123	139
11	Gly-HPO/DGMPS	BAMPO	145 °C, 3 h	195 °C, 2 h	146	136	148
12	Gly-HPO/DGMPS	APDS	120 °C, 3 h	160 °C, 3 h	120	100	118
13	Gly-HPO/BGDMSB	DDM	120 °C, 2 h	180 °C, 2 h	123	119	138
14	Gly-HPO/BGDMSB	BAMPO	145 °C, 3 h	195 °C, 3 h	145	130	148
15	Gly-HPO/BGDMSB	APDS	120 °C, 3 h	160 °C, 3 h	100	84	99

[a] For the mixtures of epoxy monomers, a 1:1 mol ratio was used.
[b] Stoichiometric amounts were used in all cases.
[c] From DSC measurements (10 °C/min).
[d] Maximum of the loss modulus from DMTA measurements.
[e] α relaxation peak of the loss factor.

Mechanical properties were measured using a dynamic mechanical thermal analysis (DMTA) apparatus (TA DMA 2928). Specimens ($3 \times 6 \times 10$ mm^3) were tested in a three point bending configuration. The thermal transitions were studied in the −100–250 °C range at a heating rate of 5 °C/min and at a fixed frequency of 1 Hz. LOI values were measured on a Stanton Redcroft, provided with an oxygen analyser, on bars of the polymers ($100 \times 6 \times 3$ mm^3).

3. Results and discussion

By using phosphorus- or silicon-containing epoxy compounds or phosphorus- or silicon-containing diamine compounds as curing agents, epoxy resins with different phosphorus or silicon contents are obtained. Based on the above, phosphorus-containing epoxy, Gly-HPO [14], and phosphorus-containing amine, BAMPO, previously described [17] are used (Scheme 1). Silicon-containing diepoxides, DGMPS [16] and BGDMSB [15] (Scheme 1) were previously synthesized by catalysed transetherification of the dimethoxymethylphenyl silane with allylic alcohol and by condensation of 1,4-bis(hydroxydimethyl silyl)benzene with allylic alcohol respectively, followed by the epoxidation of the intermediate compounds in both cases. These synthetic approaches in two steps, led to a products with moderate yields.

Alkoxysilanes are usually prepared by reaction of chlorosilanes with either alcohols or alkoxides. Since these reactions either involve acidic (evolution of HCl) or basic conditions (alkoxide, or base as HCl acceptor), alternative methods are advantageous. A particularly mild method is the alcoholysis of hydrogen-substituted silanes, because only H_2 is formed as a byproduct. However, alcohols normally do not attack silanes in the absence of a catalyst and most silanes undergo alcoholysis only in the presence of either strongly nucleophilic or electrophilic catalysts. A limited number of transition metal complexes have been reported as homogeneous catalyst for the alcoholysis of hydrosilanes. The Wilkinson catalyst, one of the more active catalysts has been used in the present work in the synthesis of DGMPS. The reaction took place at 60 °C for 1 h. The Wilkinson catalyst, like most of the transition metal complexes is not active to catalyze the alcoholysis of trialkylsilanes. On the other hand, the copper hydride complex $[(Ph_3P)CuH]_6$ is a very reactive catalyst for the alcoholysis of hydrosilanes under mild reaction conditions [18]. It provides silyl ethers in generally high yields. In this case the tertiary silane, 1,4-bis(dimethyl silyl)benzene, reacts with glycidol at room temperature for 5 h to give the corresponding silylglycidylether.

Epoxy resins have been prepared by curing with stoichiometric amounts of diamine with the compositions, phosphorus and silicon contents that are shown in Table 1. The reactions were monitored by DSC and showed exotherms with crosslinking enthalpy values and onset and maximum heat release rate temperatures collected in Table 1. Fig. 1 depicts the crosslinking exotherms for GLY-HPO with different amines (a), for the APDS amine with different epoxy compounds (b) and for the system Gly-HPO/DGMPS with different amines (c). The diamine curing agent with the lowest peak exotherm temperature under the same curing conditions was more reactive towards the epoxy resin. The APDS amine showed the highest reactivity and the BAMPO the lowest, either when reacts with pure epoxy monomer, Gly-HPO, or with a mixture of epoxy monomers, Gly-HPO/DGMPS. The reactivity may vary because of the electronic effects. An electron-donating group by resonance in the amine compound, e.g. the oxygen atom in APDS, increased the electron density of the amine groups towards oxirane ring. This effect is lower for DDM because methylene group is an electron-donating group by inductive effect. Incorporating electron-withdrawing groups such as –P═O groups in BAMPO, reduced the activity in curing epoxides.

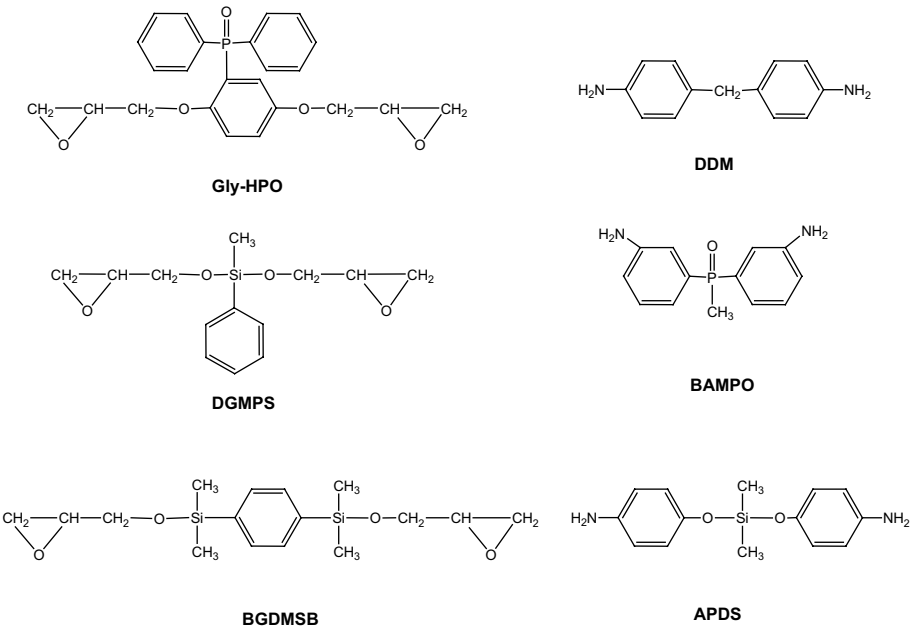

Scheme 1.

In addition, the epoxy resins with the lowest peak exothermic temperature under the same curing conditions were more reactive towards the curing agent. As can be seen in Fig. 1b Gly-HPO and DGMPS showed the highest reactivity. We previously reported [16,19] that silicon-containing oxiranes have higher reactivity due to electronic effects. The silicon atom acts as a π acceptor, withdrawing the electron density of the oxygen atom and increasing its electron-withdrawing character. Therefore, the electrophilic character of the oxirane carbons increases. The high reactivity of Gly-HPO may be also explained due to an increase in the electron-withdrawing character of the oxygen, because the resonance effect of P═O group in the ortho position to the glycidyl moiety. BGDMSB showed the lowest reactivity because the π acceptor character of the silicon atom towards oxygen atom diminishes due to the adjacent aromatic ring. Even for the systems Gly-HPO/BGDMSB which show the higher reactivity difference between epoxy monomers only an exotherm appears, thus indicating that crosslinking takes place homogeneously.

According to DSC data epoxy networks were prepared at the curing and post-curing conditions shown in Table 2. FTIR spectroscopy showed the disappearance of the absorption at 910 cm^{-1} of the oxirane ring, thus confirming that the curing reaction takes place to completion.

Table 2 also summarizes the T_gs of the crosslinked materials that can be detected as an endothermic step in the heat flow by DSC, as the maximum of the loss modulus (E'') and as the α relaxation peak of the loss factor by DMTA. As can be seen the most decisive parameter that affects the T_g value is the epoxy monomer. Higher T_g values were obtained for Gly-HPO, which contains a strong polar P═O group and a bulky pendant moiety that causes restriction in the segmental mobility. The T_g values decrease for the DGMPS epoxy thermosets, what can be explained by the presence of Si–O and Si–C units and the lower proportion of aromatic moieties in the backbone.

The T_g of thermosets from BGDMSB has the lowest T_g values that must be related to a larger volume fraction of Si–O and Si–C units in the backbone.

The mixed epoxy systems exhibit a single T_g between the T_gs of pure epoxy monomers, indicating a homogeneous morphology for these systems, in accordance with the observations of other authors [20].

The dynamic mechanical behaviour of the phosphorus- and silicon-containing epoxy resins was studied as a function of the temperature beginning in the glassy state of each composition to the rubbery plateau of each material. Fig. 2 shows the obtained plots for Gly-HPO (a), for the APDS amine (b) and for the system Gly-HPO/DGMPS (c). The crosslinking density of a polymer can be estimated from the plateau of the elastic modulus in the rubbery state [21]. This theory is strictly valid for lightly crosslinked materials, and was therefore used to make qualitative comparisons of the crosslinking density among the various polymers. As can be seen in Fig. 2 for the crosslinking of Gly-HPO, the lower crosslinking density is obtained when APDS is used as a curing agent. As far as the chemical structures of these networks are concerned, this behaviour is to be expected since longer Si–O and Si–C bonds should provide flexibility to the backbone. A similar trend can be observed for the systems Gly-HPO/DGMPS. When comparing the crosslinking density of the epoxy monomers cured with APDS (Fig. 2b), it can be seen that the lower crosslinking density is achieved for DGMPS, which contains additional Si–O and Si–C units that confer flexibility to the network.

The plots of loss factor versus temperature show the α relaxation peak, which is associated with the T_g of the materials and follows the trend mentioned earlier. Moreover, the analysis of the height and width of the α relaxation peak shows trends in the crosslinking densities and network homogeneities. The height of the tan δ peak decreases for the APDS crosslinked systems. Because tan δ is the ratio of viscous component to elastic component, it can be assumed that the decreasing height is associated with lower segmental mobility and fewer relaxing species, and is therefore indicative that networks for the APDS containing systems show higher flexibility. The peak width at half height broadens as the number of branching modes increases, which produces a wider distribution of structures. The range of temperatures at which the different network segments gain mobility therefore increases. There were no significant differences among the different samples, thus showing similar branching distribution for all samples.

To examine the effect of phosphorus and silicon content on thermal stability and the decomposition behaviour, TGA data under nitrogen and air atmospheres were determined and analyzed. Fig. 3 shows the weight loss with the temperature for some of the epoxy

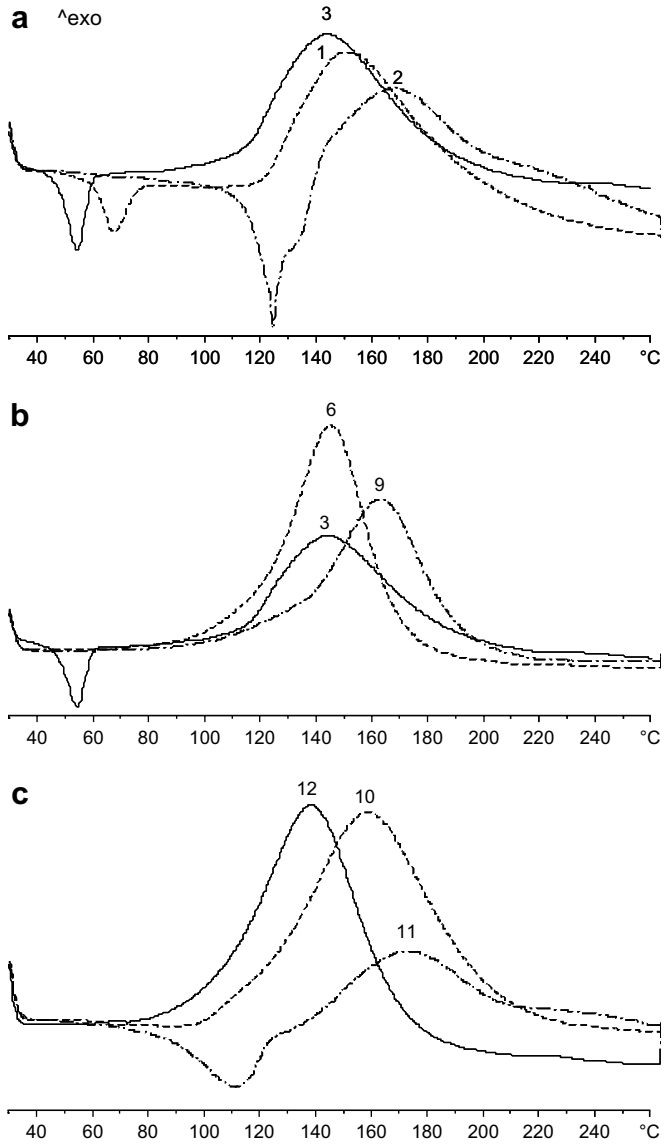

Fig. 1. DSC plots of systems (a) 1 (Gly-HPO/DDM), 2 (Gly-HPO/BAMPO) and 3 (Gly-HPO/APDS); (b) 3 (Gly-HPO/APDS), 6 (DGMPS/APDS) and 9 (BGDMSB/APDS); (c) 10 (Gly-HPO/DGMPS/DDM), 11 (Gly-HPO/DGMPS/BAMPO) and 12 (Gly-HPO/DGMPS/APDS).

compositions. Table 3 summarizes the thermogravimetric data. Decomposition temperatures ($T_{5\%}$) for the phosphorus-containing resins are lower than for the conventional epoxy resins due to the decomposition of P–C bonds which have lower thermal stability than C–C bonds [22]. Moreover, decomposition temperatures for the silicon-containing resins are also expected to be lower than conventional epoxy resins. The Si–O unit can decompose at lower temperatures leading to the formation of the silicone-containing group [16]. In our case, independent of the atmosphere, all the thermosets start the degradation at similar temperatures, being slightly lower in air. No relationships between decomposition temperatures and phosphorus or/and silicon contents can be established.

In nitrogen, two different behaviours can be observed. Some samples exhibit a single major break in their decomposition curve before their major weight losses level off. This behaviour is indicative of a single mechanism of decomposition which is similar for these resins. The others show a two step break in the decomposition curves, suggesting a more complex decomposition pathway.

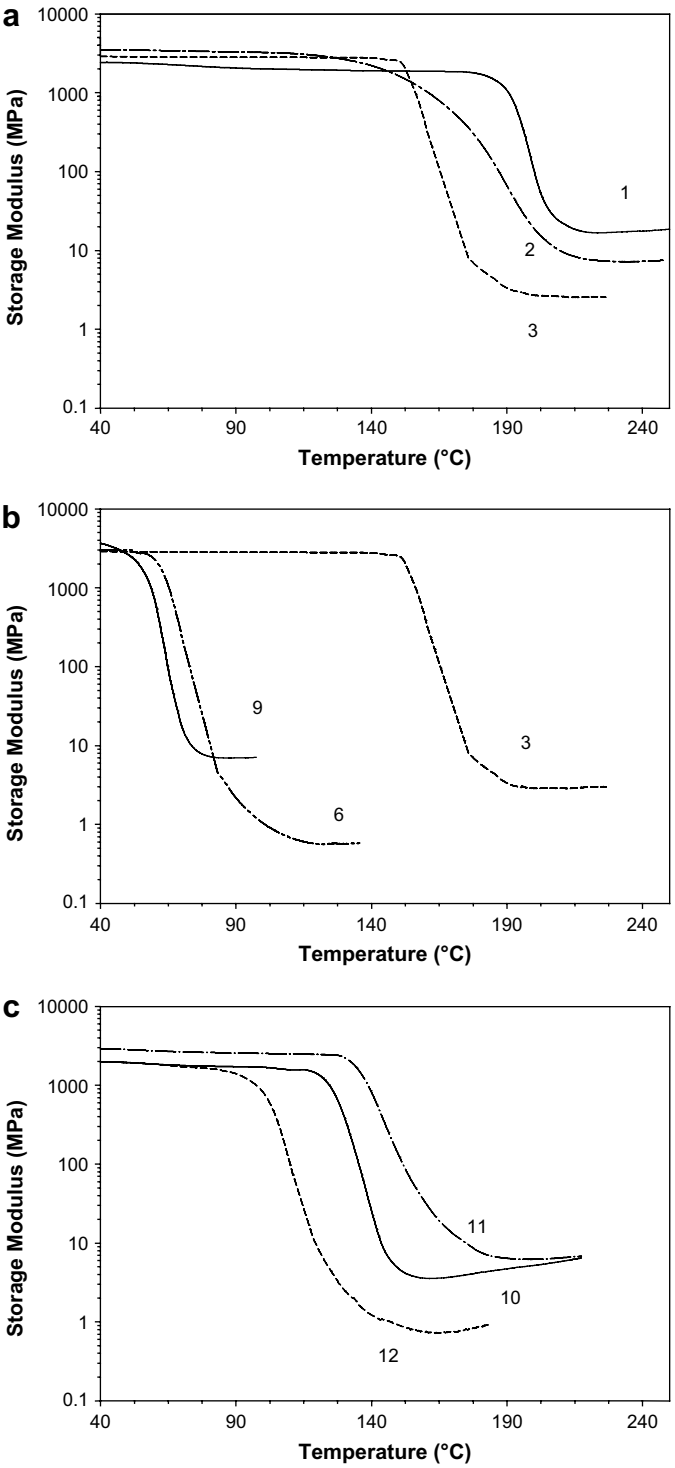

Fig. 2. Storage modulus for (a) 1 (Gly-HPO/DDM), 2 (Gly-HPO/BAMPO) and 3 (Gly-HPO/APDS); (b) 3 (Gly-HPO/APDS), 6 (DGMPS/APDS) and 9 (BGDMSB/APDS); (c) 10 (Gly-HPO/DGMPS/DDM), 11 (Gly-HPO/DGMPS/BAMPO) and 12 (Gly-HPO/DGMPS/APDS).

Again, no relationships can be established. In air a third stage in the decomposition process is observed at temperatures above 500 °C. Under an air atmosphere, the weight loss of a polymeric material at these temperatures came from the oxidation of the formed char. According to the mechanism of improved fire performance via phosphorus incorporation, the phosphorus groups form an insulating protective layer which prevents the volatiles from

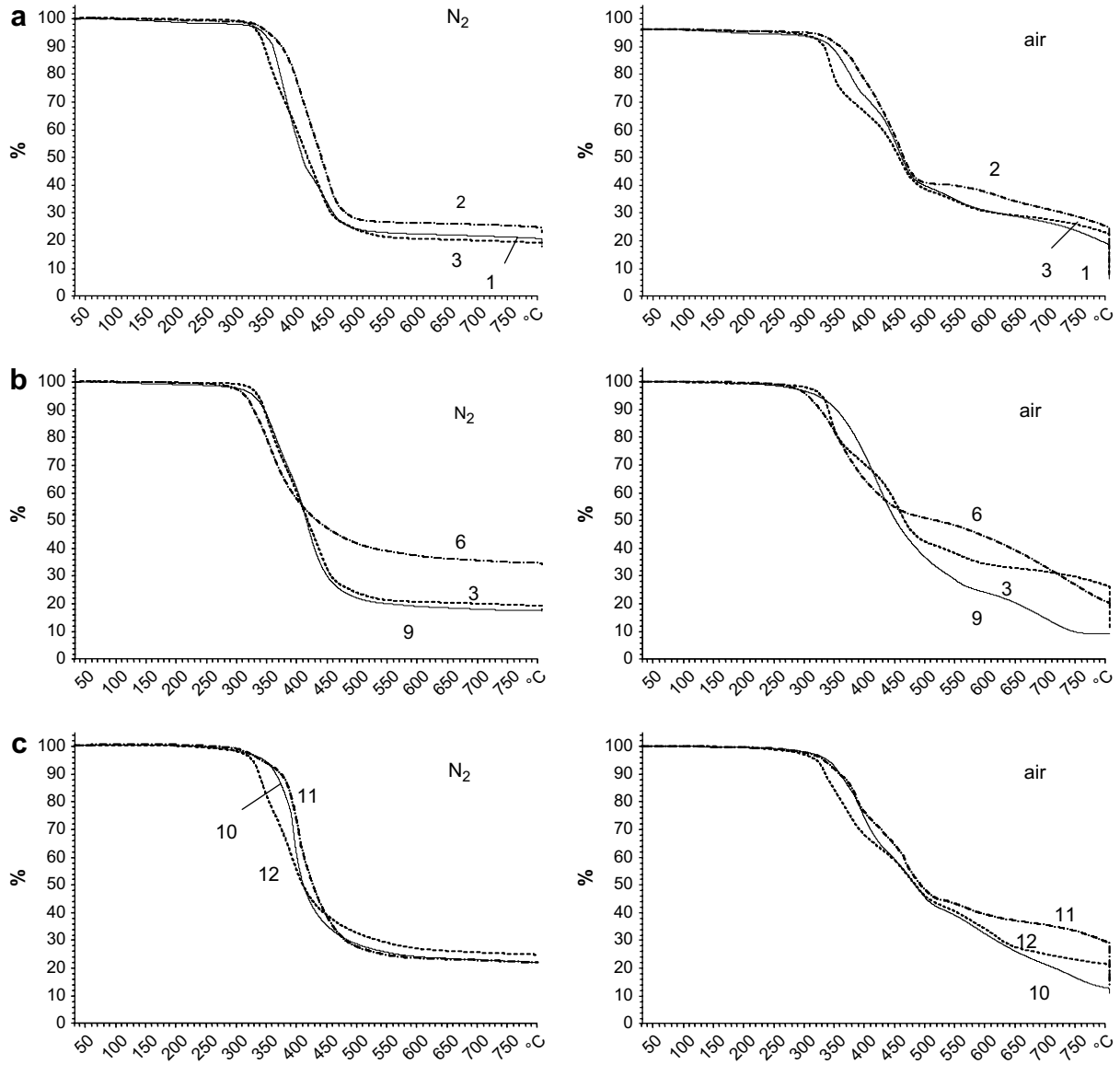

Fig. 3. TGA plots in nitrogen and air for (a) 1 (Gly-HPO/DDM), 2 (Gly-HPO/BAMPO) and 3 (Gly-HPO/APDS); (b) 3 (Gly-HPO/APDS), 6 (DGMPS/APDS) and 9 (BGDMSB/APDS); (c) 10 (Gly-HPO/DGMPS/DDM), 11 (Gly-HPO/DGMPS/BAMPO) and 12 (Gly-HPO/DGMPS/APDS).

Table 3
Thermogravimetric data of epoxy resins

Sample	P (%)	Si (%)	Nitrogen				Air					LOI $\%O_2$ (V/V)
			$T_{5\%}$[a] (°C)	T_{m1}[b] (°C)	T_{m2}[b] (°C)	Char[c] (%)	$T_{5\%}$[a] (°C)	T_{m1}[b] (°C)	T_{m2}[b] (°C)	T_{m3}[b] (°C)	Char[c] (%)	
1	5.9	–	345	390	430	23	338	383	456	550	22	31.0
2	8.5	–	352	410	450	25	352	393	458	560	29	32.0
3	5.5	2.5	335	350	435	20	328	342	460	630	27	31.0
4	–	7.7	318	–	415	34	302	325	412	580	16	36.0
5	4.0	7.2	308	–	430	33	312	380	470	750	31	38.0
6	–	10.4	320	350	–	35	306	356	–	745	22	37.0
7	–	12.8	362	–	439	21	348	419	–	690	12	33.5
8	3.4	12.2	358	–	420	15	307	416	–	680	11	33.9
9	–	14.7	329	362	420	18	320	430	–	700	9	33.0
10	3.5	3.2	336	–	400	23	338	380	470	595	13	36.5
11	6.6	3.0	341	–	406	24	332	385	460	560	31	34.0
12	3.2	5.8	327	340	390	25	319	350	478	575	22	34.6
13	3.2	5.8	330	–	400	19	302	390	470	600	9	34.0
14	6.2	5.5	331	395	447	16	323	380	475	564	24	33.5
15	3.0	8.1	317	355	–	17	304	420	480	605	16	33.6

[a] Temperature of 5% weight loss.
[b] Temperature of the maximum weight loss rate.
[c] Char yield at 800 °C.

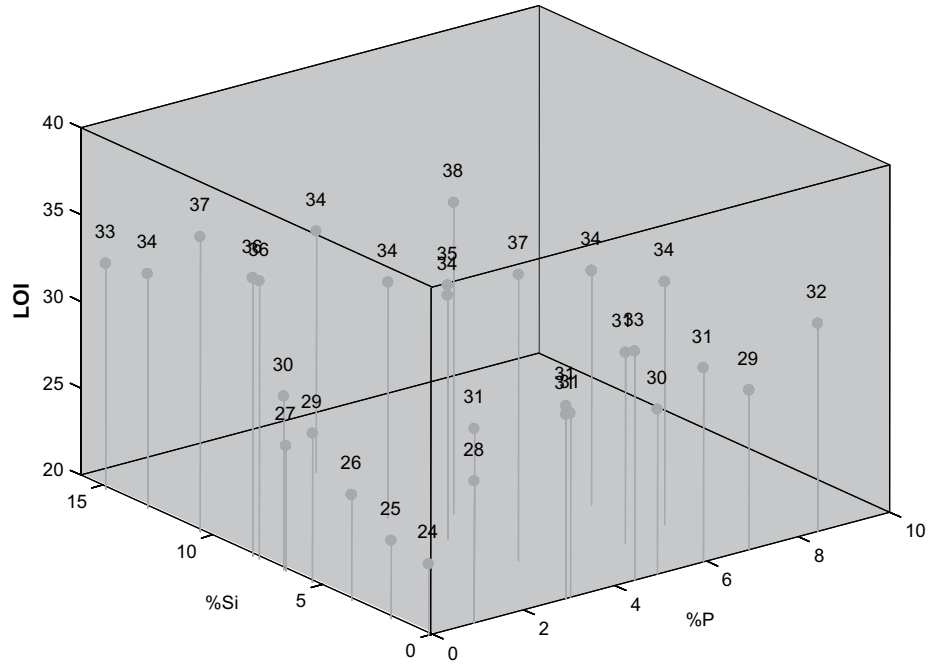

Fig. 4. Plot of LOI values for phosphorus-, silicon- and phosphorus–silicon-containing epoxy resins.

transferring to the surface of the materials and increases the thermal stability of the char at higher temperatures. Silicon-containing polymers are described that can degrade forming thermally stable silica, which have the tendency to migrate to the char surface serving as a protection layer to prevent further degradation of char at high temperatures [8]. For the P–Si synergistic effect of flame retardation, it has been described that phosphorus provides a tendency for char formation and silicon favorably provides an enhancement of the thermal stability of the char, resulting in a high efficiency of char formation which exhibits extremely high thermal stability and antioxidant properties. In our case, no increase in the amount of char yield in air at 800 °C with the P + Si content was observed.

The LOI values of the phosphorus–silicon-containing epoxy resins are shown in Table 2. Materials with outstanding LOI values are obtained, with the corresponding excellent flame retardant properties. Fig. 4 depicts LOI values for phosphorus- [14,23], silicon- [15,16] and phosphorus–silicon-containing epoxy resins. As we described previously, it can be observed that the presence of phosphorus in phosphorus-containing epoxy resins increases the LOI values even when the phosphorus content is low, and no significant differences with the phosphorus content are observed. For the silicon-containing epoxy resins, the LOI values increase with increasing silicon content up to contents of 10%. However, a synergistic effect cannot be observed for phosphorus–silicon-containing epoxy resins and significant improvements in LOI values are not reached.

4. Conclusions

The curing of phosphorus- and silicon-containing epoxy monomers with conventional DDM and phosphorus- and silicon-containing amines was studied by DSC. The most reactive monomer was DGMPS and the most reactive curing agent was APDS because of the electronic effects. The thermal and flame retardant properties were evaluated. Materials with outstanding LOI values are obtained, with the corresponding excellent flame retardant properties that could bring some benefits to the epoxy resins in applications. A synergistic effect cannot be observed for phosphorus–silicon-containing resins.

Acknowledgements

The authors express their thanks to CICYT (Comisión Interministerial de Ciencia y Tecnología) (MAT2005-01593) for providing financial support for this work.

References

[1] May CA, editor. Epoxy resins chemistry and technology. New York: Marcel Dekker; 1988.
[2] Kinjo N, Ogata M, Nishi K, Kaneda A. Adv Polym Sci 1989;88:1.
[3] Hamerton I, Lu SY. Prog Polym Sci 2002;27:1661.
[4] Levchik SV, Weil ED. Polym Int 2004;53:1901.
[5] Weil E, Levchik SV. J Fire Sci 2004;22:25.
[6] Green J. In: Grand AF, Wilkie CA, editors. Fire retardancy of polymeric materials. New York: Marcel Dekker; 2000.
[7] Ebdon JR, Jones MS. In: Salomone JC, editor. Polymeric materials encyclopedia. Boca Raton: CRC Press; 1992.
[8] Kashiwagi T, Gilman JW. In: Grand AF, Wilkie CA, editors. Fire retardancy of polymeric materials. New York: Marcel Dekker; 2000.
[9] Liu YL, Chiu CI. Polym Degrad Stab 2005;90:515.
[10] Khurana P, Narula AK, Choudhary V. J Appl Polym Sci 2003;90:1739.
[11] Wu CS, Liu YL, Chiu YS. Polymer 2002;43:4277.
[12] Hsiue GH, Liu YL, Tsiao J. J Appl Polym Sci 2000;78:1.
[13] Hsiue GH, Liu YL, Liao HH. J Polym Sci Part A Polym Chem 2001;39:986.
[14] Spontón M, Ronda JC, Galià M, Cádiz V. J Polym Sci Part A Polym Chem 2007;45:2142.
[15] Mercado LA, Galià M, Reina JA. Polym Degrad Stab 2006;91:2588.
[16] Mercado LA, Reina JA, Galià M. J Polym Sci Part A Polym Chem 2006;44:5580.
[17] Mercado LA, Ribera G, Galià M, Cádiz V. J Polym Sci Part A Polym Chem 2006;44:1676.
[18] Brestensky DM, Huseland DE, McGettigan C, Stryker JM. Tetrahedron Lett 1988;29:3749.
[19] Mercado LA, Galià M, Reina JA, Garrido M, Larrechi MS, Rius FX. J Polym Sci Part A Polym Chem 2006;44:1447.
[20] Wang WJ, Perng LH, Hsiue GH, Chang FC. Polymer 2000;41:6113.
[21] Tobolsky AV, Carlson DW, Indictor NJ. J Polym Sci 1961;54:175.
[22] Quittmann U, Lecamp L, El Khatib W, Youssef B, Bunel C. Macromol Chem Phys 2001;202:628.
[23] Ribera G, Mercado LA, Galià M, Cádiz V. J Appl Polym Sci 2006;99:1367.